# Deep oceanic zonal jets constrained by fine-scale wind stress curls in the South Pacific Ocean: A high-resolution coupled GCM study

B. Taguchi,[1] R. Furue,[2] N. Komori,[1] A. Kuwano-Yoshida,[1] M. Nonaka,[3] H. Sasaki,[1] and W. Ohfuchi[1]

Received 7 February 2012; revised 12 March 2012; accepted 12 March 2012; published 24 April 2012.

[1] Oceanic alternating zonal jets at depth have been detected ubiquitously in observations and ocean general circulation models (GCMs). Such oceanic jets are generally considered as being generated by purely oceanic processes. Here we explore a possible air-sea interaction induced by surface signatures of the deep zonal jets using an eddy-permitting coupled atmosphere-ocean GCM (CGCM). The 23-year CGCM integration reproduces bands of latitudinally-narrow alternating jets in the Southeast Pacific. They extend from the sea surface to well below the main thermocline and are embedded in the large-scale westward-flowing South Equatorial Current, the latter mostly confined above the thermocline. These jets generate fine-scale sea surface temperature (SST) anomalies through the advection of zonal temperature gradients. The atmospheric boundary layer appears to respond thermally to this fine-scale SST field, which induces fine-scale wind stress anomaly through atmospheric pressure adjustment, as indicated by a good spatial correlation between the SST Laplacian field and the fine-scale wind stress curl. A Sverdrup calculation on the wind stress field of the CGCM predicts fine-scale zonal currents driven by the meridional gradient of the fine-scale wind stress curl. The positions of these Sverdrup currents are generally coincident with those of the original zonal jets and the Sverdrup prediction explains roughly half of the amplitudes of the jets. While the original cause of the deep zonal jets simulated in our CGCM is unidentified, this analysis suggests that there is likely a positive air-sea feedback: the jets generate fine-scale wind stress curl that reinforces themselves through the Sverdrup dynamics.
**Citation:** Taguchi, B., R. Furue, N. Komori, A. Kuwano-Yoshida, M. Nonaka, H. Sasaki, and W. Ohfuchi (2012), Deep oceanic zonal jets constrained by fine-scale wind stress curls in the South Pacific Ocean: A high-resolution coupled GCM study, *Geophys. Res. Lett.*, *39*, L08602, doi:10.1029/2012GL051248.

## 1. Introduction

[2] Oceanic alternating zonal jets at depth with the meridional scales of 3–5° have been detected ubiquitously in observations [*Maximenko et al.*, 2005, 2008] and ocean general circulation models (OGCMs) [*Nakano and Hasumi*, 2005; *Richards et al.*, 2006, 2008]. As *Nakano and Hasumi* [2005] were able to simulate the deep zonal jets with a high-resolution OGCM driven by spatially smoothed wind forcing, it is expected that the oceanic jets can be generated by purely oceanic processes such as geostrophic turbulence, PV-staircases, and $\beta$-plume forced by local forcings [e.g., *Melnichenko et al.*, 2010, and references therein]. On the other hand, *Kessler and Gourdeau* [2006, hereinafter KG06] provided another view of the "wind-driven" oceanic zonal jets. Specifically, they analyzed climatological geostrophic currents based on hydrography to find bands of meridionally-narrow, eastward, deep currents under the main thermocline, the latter sustaining the large-scale westward flow of the South Pacific subtropical gyre. Surprisingly, on vertical integration those fine-scale currents were consistent with zonal jets in a Sverdrup calculation on satellite-observed wind stress.

[3] The time-mean vorticity balance of depth-integrated flows can generally be considered as the sum of linear Sverdrup dynamics and nonlinear effects as described by *Kessler et al.* [2003]:

$$V = (\beta\rho)^{-1} curl(\tau + \tau^{NL}) \tag{1}$$

$$U = -(\beta\rho)^{-1} \int_{x_E}^{x} \left[\partial curl(\tau + \tau^{NL})/\partial y\right] dx' \tag{2}$$

where $U$ and $V$ are the zonal and meridional transports per unit width; $\rho$ is a mean density of the sea water; $\beta$ is the meridional gradient of the Coriolis parameter; $\tau$ is the wind stress vector; $x_E$ is the eastern limit of zonal integration, taken here as 90°W; $\tau^{NL}$ represents all the nonlinear terms of the momentum equations; and bottom stress is ignored. Note that the continuity equation is used to derive equation (2) from equation (1) and that $dx'$ in equation (2) is negative as the integration goes westward. While earlier studies focusing on oceanic internal processes attributed the generation of oceanic fine-scale structures such as deep jets entirely to the nonlinear stress $\tau^{NL}$, KG06 demonstrated that some of the oceanic fine-scales are driven by fine-scale structures in curl $\tau$. The cause of such fine scales in wind stress, however, remains unknown.

[4] Zonal jets are often found leeward of islands induced by their blockage of planetary waves [*Webb*, 2000; *Qiu et al.*, 2009] or driven by dipolar wind curls produced in the lee of islands with high mountains [*Xie et al.*, 2001; *Chelton et al.*, 2004]. While the mountain-generated dipoles and resulting oceanic jets are associated with fine-scale wind curls, it is yet to be understood what give rise to such fine-scale wind stress curl structure over the Central South

[1]Earth Simulator Center, Japan Agency for Marine-Earth Science and Technology, Yokohama, Japan.
[2]International Pacific Research Center, University of Hawai'i at Mānoa, Honolulu, Hawaii, USA.
[3]Research Institute for Global Change, Japan Agency for Marine-Earth Science and Technology, Yokohama, Japan.


0094-8276/12/2012GL051248

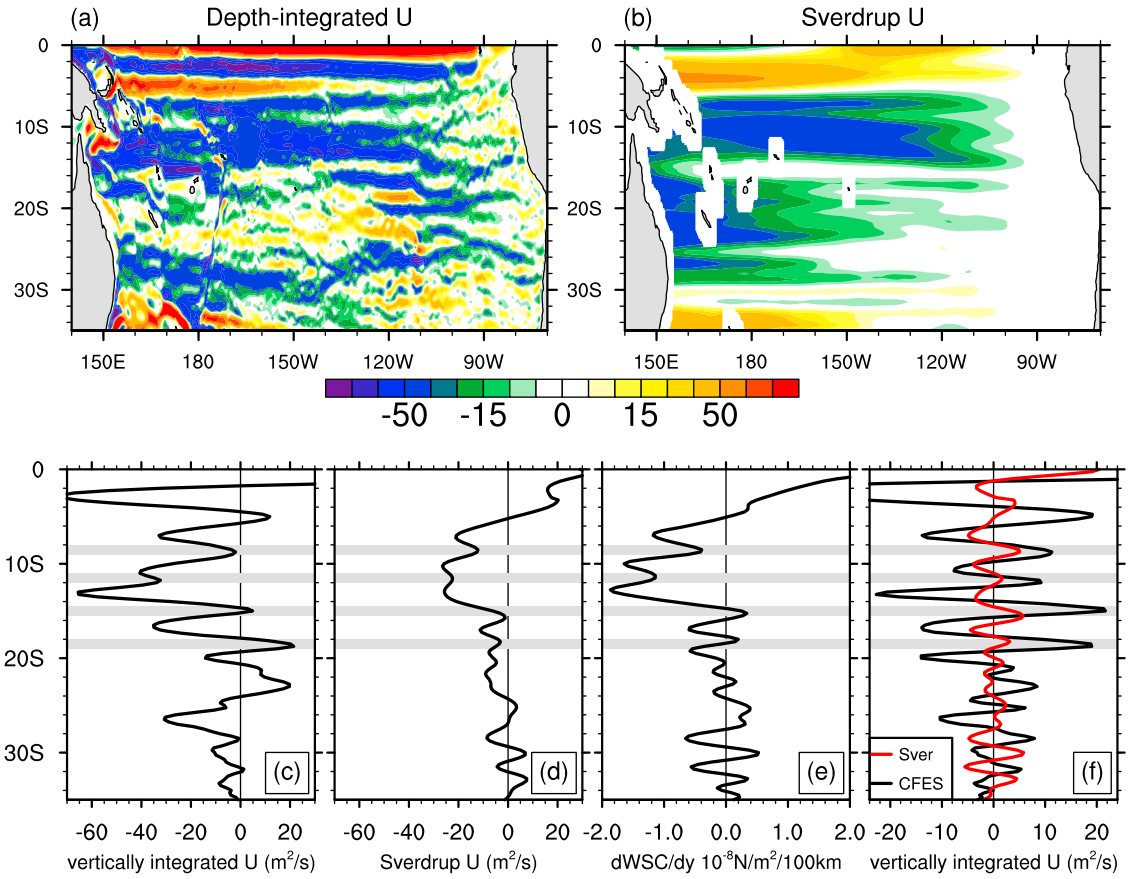


**Figure 1.** (a) Depth-integrated zonal velocity for the subtropical South Pacific domain. (b) Sverdrup flow by equation (2). (c) Meridional profile of vertically-integrated zonal velocity zonally averaged over 150°–110°W. (d) As in Figure 1c but Sverdrup transport computed from the annual mean wind stress curl. (e) Meridional gradient of the wind stress curl averaged over 130°–100°W. (f) Latitudinally high-pass filtered vertically-integrated zonal velocity (black) and Sverdrup transport (red). All these quantities are averaged over years 17–20 of the CFES integration.

Pacific ocean without any prominent island blockages to the east. Here we put forward a hypothesis that the fine-scale wind curl is an atmospheric boundary layer (ABL) response to fine-scale sea surface temperature (SST) anomaly that is generated by the oceanic barotropic zonal jets. The objective of this study is to explore this possible air-sea interaction between the oceanic zonal jets and the fine-scale wind curls using a high-resolution coupled atmosphere-ocean GCM (CGCM) and to quantify how much of the simulated oceanic fine-scales are driven by fine-scale wind curls in the South Pacific.

## 2. A High-Resolution CGCM and Observational Data

[5] The model used in this study is "CFES," the CGCM for the Earth Simulator (ES) [*Komori et al.*, 2008a, 2008b]. CFES has been integrated for 23 years with horizontal resolutions of T239 spectral truncation (equivalently 50-km grid intervals) for its atmospheric component [*Enomoto et al.*, 2008; *Kuwano-Yoshida et al.*, 2010], and 0.25° grid intervals for its oceanic component [*Komori et al.*, 2005]. The atmospheric model has 48 vertical levels, the ocean model 54. CFES uses the traditional coupling scheme where the ocean surface velocity is not taken into account when calculating air-sea momentum fluxes. In reality, wind stress curl can be generated from both the atmospheric and oceanic surface velocity fields but our coupling scheme eliminates the latter effect. To extract fine-scales, two-dimensional Hann filter with a half-width of 4° is applied twice to field variables following *Maximenko et al.* [2008].

[6] For observational reference, we use geostrophic currents computed relative to 2000-m based on climatological mean temperature and salinity fields from Argo float observations. The Argo climatology used in this study is "the IPRC Argo Dataset" [*Lebedev et al.*, 2010], which is analyzed on a 1° × 1° grid on standard levels using a variational technique (available from the IPRC/APDRC, Univ. of Hawaii at http://apdrc.soest.hawaii.edu/projects/argo/).

## 3. Deep Zonal Jets Simulated in CGCM

[7] The simulated oceanic fine-scale flows exhibit both quasi-stationary and propagating features (See Section 5, Figure 4a). In this section, we show CFES results for the period of 17–20th model year, a period when the quasi-stationary feature dominates. Figure 1a and Figure S1 in the auxiliary material show the vertically-integrated zonal velocity $U_{int}$ averaged over the 17–20th years of the

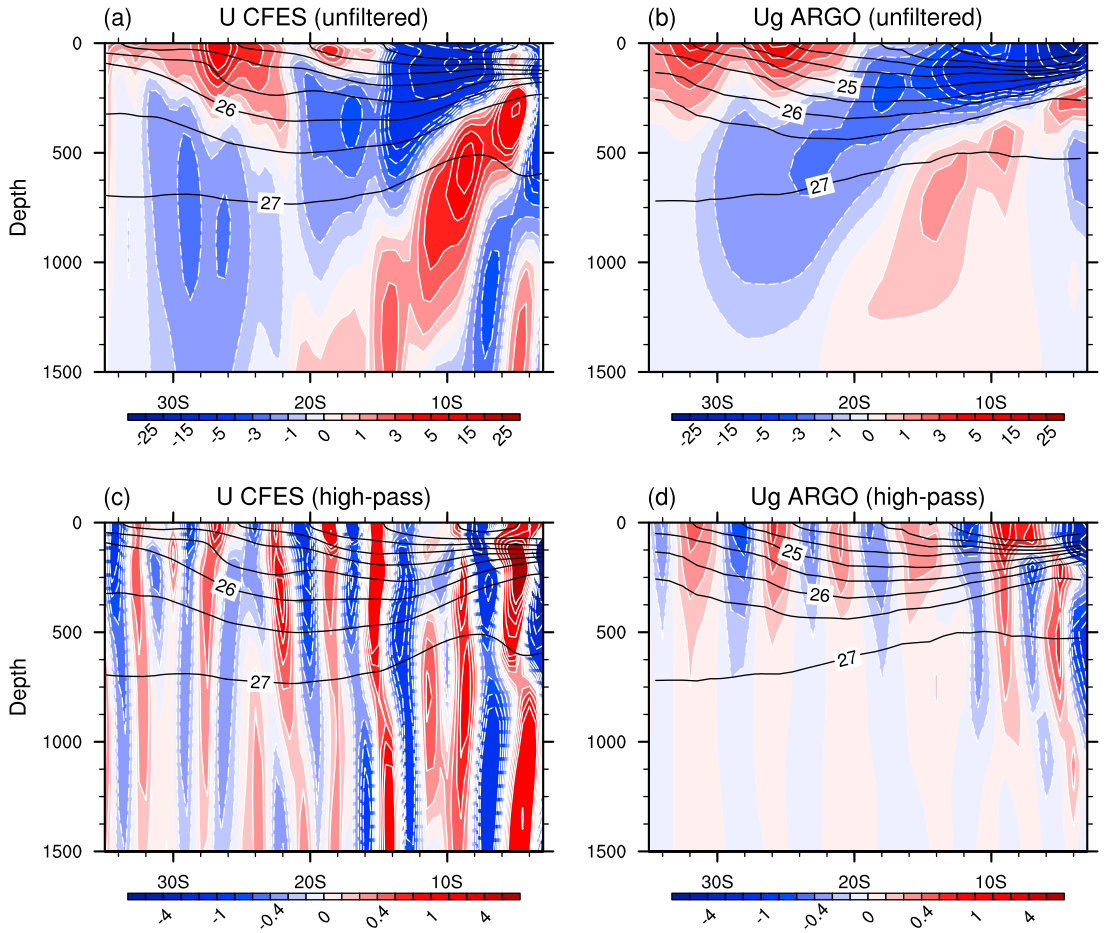


**Figure 2.** (a) Latitude-depth section of zonal velocity (color shading with white contours; unit in cm $s^{-1}$) and potential density $\sigma_\theta$ (black contours; unit in kg $m^{-3}$) averaged over 160°–130°W and years 17–20 of the CFES integration. (b) As in Figure 2a but a geostrophic calculation on an Argo climatology assuming the level of no motion at 2000 m depth. (c, d) As in Figures 2a and 2b but the spatially high-pass filtered zonal velocity.

CFES integration, for the subtropical South Pacific and global domains, respectively.[1] An eddy permitting resolution (0.25°) of CFES's ocean component is high enough to reproduce zonally striated structures almost everywhere in the world ocean (Figure S1), although they are possibly weaker than those simulated in higher-resolution models [*Nakano and Hasumi*, 2005]. Particularly prominent are latitudinally-narrow eastward currents and minima in westward velocity embedded in large-scale westward flows in the equatorward sides of subtropical gyres. The rest of the paper focuses on the zonal jets in the subtropical south Pacific, which appear to reside well east of major island groups of the southwest Pacific, where conventional island-induced jets [*Webb*, 2000; *Qiu et al.*, 2009] or eastward countercurrents induced by dipolar wind curls [*Xie et al.*, 2001; *Chelton et al.*, 2004] are not expected to occur.

[8] Figure 2 compares zonal velocity between the CFES simulation and the geostrophic calculation from Argo (section 2); for the plots, the same zonal sector (160°–130°W) as KG06's is chosen. The Argo climatology captures zonal currents that have maximum eastward velocity cores around 3°S, 9°S, and 15°S below the main thermocline, which shoals equatorwards in the subtropical South Pacific and sustains the broad-scale westward-flowing South Equatorial Current (SEC). This vertical structure is generally consistent with the KG06's analysis (KG06, Figure 5) based on the World Ocean database. Similar deep zonal currents are found in the CFES integration, although cores of the simulated flows are located at 5°S, 8°S, 12°S, and 15°S, not exactly the same as in the observational counterparts. Nevertheless, the vertical structure of the simulated zonal flows are similar to those in observations in that the maximum eastward velocity cores exist below the main thermocline and that the depth of the cores increases poleward.

[9] High-pass filtering (Figures 2c and 2d) reveals vertically-coherent, alternating zonal jets, which extend up to the surface in both CFES and the Argo climatology. The vertical coherency of fine-scale jets may arise from the barotropization of mesoscale eddies through the vertical momentum transfer by interfacial form drag [e.g., *Vallis*, 2006]. Our analysis suggests that the eastward currents below the main thermocline described by KG06 can be viewed as a superposition of the large-scale flow (shallow westward flow and weaker eastward flow underneath) and latitudinally narrow and vertically coherent alternating jets, leading to the apparent eastward-current

[1]Auxiliary materials are available in the HTML. doi:10.1029/2012GL051248.

cores below the thermocline. The large-scale baroclinic flow that deepens poleward may be driven by upwelling along the coast of South America (KG06) or by the damping of higher-mode Rossby waves as in *Nakano and Hasumi* [2005]. Due to the superposed large-scale flow, the alternating jets in the South Pacific are less obvious in the total field than those shown in an eddy-resolving OGCM [*Richards et al.*, 2008] and in an ocean reanalysis [*Divakaran and Brassington*, 2011], where deep jets are apparent in the unfiltered fields.

[10] Next, we examine the degree to which the depth-integrated zonal currents are explained by the wind-driven Sverdrup dynamics. The zonal component of the Sverdrup flow (Figure 1b) is computed as $U_{SV} = -(\beta\rho)^{-1} \int_{x_E}^{x} [\partial\, curl(\tau)/\partial\, y]dx'$ where the wind stress field $\tau$ is taken from the CFES output. The zonally averaged meridional structure of the zonal jets in the central basin of the South Pacific (Figure 1c), is reasonably well represented by that of the Sverdrup flow (Figure 1d). Namely, fine-scale alternating jets embedded in the large-scale westward flow are well aligned each other between $U_{int}$ and $U_{SV}$ with their peaks in eastward transport located at about 9, 12, 15, and 19°S (gray stripes). Comparing the fine-scale (high-pass filtered) components of $U_{int}$ and $U_{SV}$ (Figure 1f) indicates that the latitudinal phase correspondence is particularly good between 8° and 20°S, where the magnitudes of Sverdrup transport explains at most 50% of the simulated depth-integrated velocity. The part of the jet transport unexplained by the wind-driven Sverdrup balance must be maintained by nonlinear stress (or bottom stress) as indicated by equation (2).

## 4. Surface Signatures and Atmospheric Influence of Deep Jets

[11] We now trace back the forcing of the banded structures found in the Sverdrup transport. Peaks in the eastward Sverdrup transport in the central South Pacific basin are primarily driven by the meridional gradients of the wind stress curl in the region slightly to the east. Figures 1d and 1e demonstrate this property: Fine-scale eastward (westward) anomalies in the zonal Sverdrup flow averaged over 150°–110°W (Figure 1d) correspond well to the positive (negative) anomalies of the meridional gradient of wind stress curl averaged over 130°–100°W (Figure 1e) within latitudinal bands shown with light gray stripes. The wiggles of wind stress curl gradient originates from the meridionally fine-scale wind stress curl itself (not shown).

[12] What then gives rise to such a fine-scale wind stress curl structure? With the typical synoptic scale (~1000 km) of the subtropical atmosphere and no obvious islands or seamounts (not shown) to the east, the fine-scale wind stress curl structure is likely due to a local fine-scale SST structure, the latter possibly being a surface signature of the oceanic deep zonal jets. Our analysis of fine-scale surface velocity, SST, and wind stress curl fields (Figure 3) strongly supports the hypothesis. The oceanic jets have meridionally fine-scale anomalies in zonal velocity of 2–3 cm $s^{-1}$ at the surface (Figures 2c and 2d; black contours in Figure 3a). These zonally-oriented anomalies (black contours in Figure 3a) are spatially in-phase with fine-scale SST anomalies (shading in Figure 3a), indicative of the advection by the fine-scale oceanic flow of the large-scale SST (Figure S2), which decreases eastward (purple contours in Figure 3a). The Laplacian of the SST (shading in Figure 3b) is largely a mirror image of the high-pass filtered SST field (shading in Figure 3a) and it turns out to be spatially well correlated with the fine-scale wind stress curl field (shading in Figure 3c; spatial correlation coefficient 0.59 for the region 20°–10°S, 140°–100°W).

[13] Note that cyclonic (anticyclonic) wind curl is collocated with positive (negative) SST anomaly (Figures 3a and 3c). This fact suggests that the fine-scale SST anomalies are not generated locally by the fine-scale wind curl. If the wind were the cause of the SST anomaly, cyclonic (anticyclonic) wind curl would induce Ekman upwelling (downwelling), leading to negative (positive) SST anomaly. Rather, the relationship between the two is consistent with the ABL response to SST anomalies via the pressure adjustment mechanism as the following simple ABL model illustrates [*Lindzen and Nigam*, 1987; *Minobe et al.*, 2008]:

$$\frac{\epsilon^2+f^2}{f}(v_x-u_y) = -\frac{\epsilon^2+f^2}{\epsilon}(u_x+v_y) = \frac{1}{\rho_a}\nabla^2 p \sim -\nabla^2 \mathrm{SST} \quad (3)$$

where $u$ and $v$ are surface wind velocity in zonal and meridional directions, respectively; subscripts $x$ and $y$ are the derivatives along the respective directions; $\epsilon$ is a damping coefficient; $p$ is atmospheric pressure; and $\rho_a$ is the ABL density.

[14] The in-phase relationship between the SST Laplacian and the fine-scale wind stress curl (Note $f < 0$ for the Southern hemisphere in equation (3)) can be found not only in the time mean map but also in the joint probability density function (PDF) for the two variables based on the 48 monthly-mean data (Figure 3d). In particular, the PDF of wind curl has a large positive (negative) bias when the SST Laplacian is strongly positive (negative) and these two PDFs are well separated from each other (Figure 3e). Besides the pressure adjustment mechanism, the vertical mixing mechanism is another well-known ABL response to SST anomalies [e.g., *Chelton and Xie*, 2010]. The CFES results, however, do not show a relationship between wind stress curl and SST gradients consistent with the latter mechanism (Figure S3). It is an interesting subject of future study to explore what determines the mode of the ABL response to fine-scale SST anomalies in this region.

## 5. Transient Features

[15] *Richards et al.* [2006, 2008] found that jet-like structures in the subtropics are dominated by features propagating towards the equator in high-resolution OGCMs, while KG06 have reported the fine-scale wind curl field that drives the Sverdrup jets to be quasi-permanent during the 1992–2004 period. CFES reproduces both quasi-steady jets and propagating ones in the central South Pacific (Figure 4a), the latter most discernible between 10° and 20°S (as indicated by black lines). Equatorward phase speeds range from 0.18 cm $s^{-1}$ to 0.56 cm $s^{-1}$ as consistent with *Richards et al.* [2006, 2008]. The general agreement between the simulated jets and Sverdrup transports seen in the time-mean field (Figures 1c and 1d) is noticeable also in the transients. Namely, a Sverdrup calculation displays the

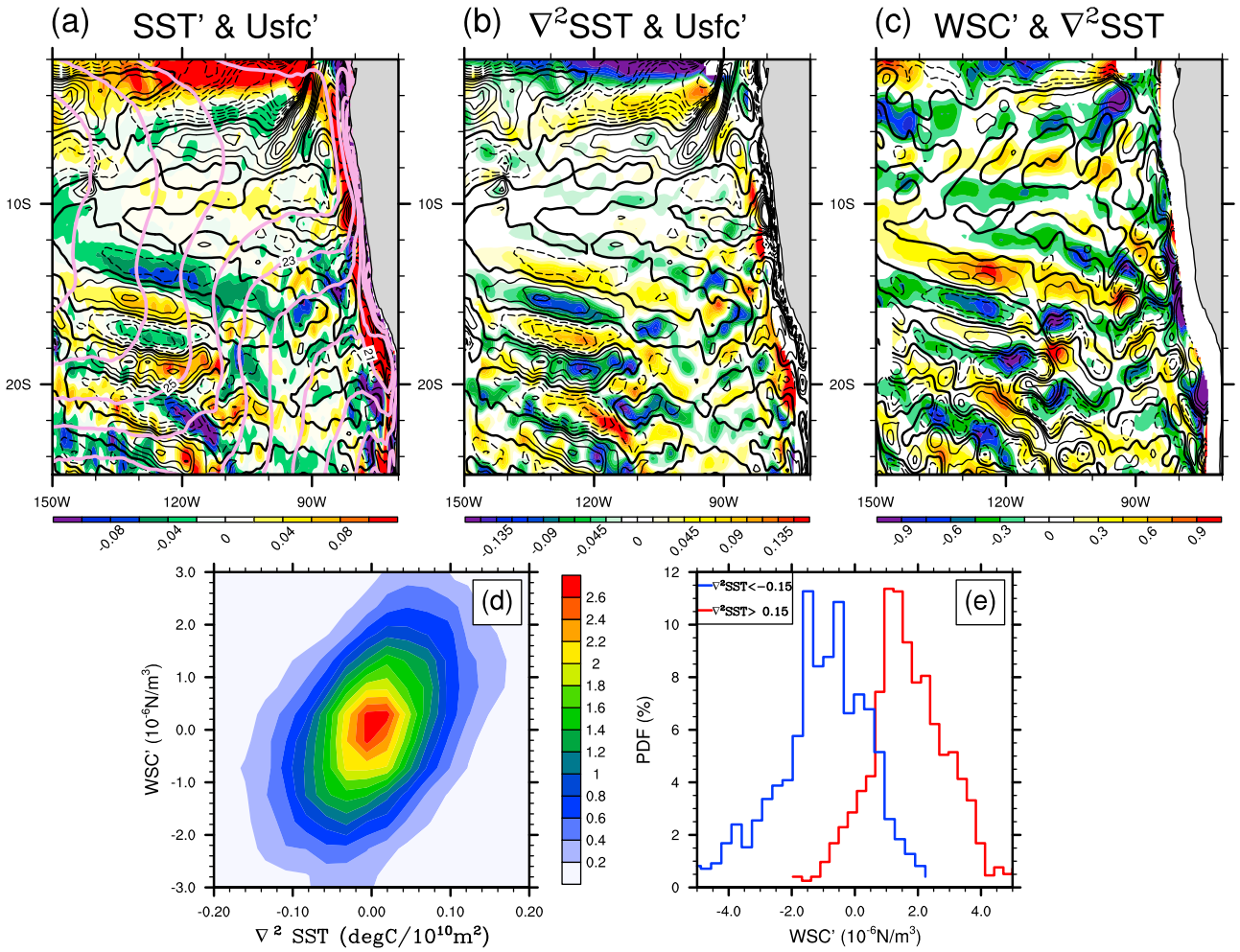


**Figure 3.** (a) SST (shading; Unit in C°), surface velocity anomalies (contours; cm $s^{-1}$) and background SST field (purple contours; C°), (b) SST Laplacian $\nabla^2$SST (shading; $10^{-10}$C°$m^{-2}$) and surface velocity anomalies (contours), (c) Wind stress curl (shading; $Nm^{-3}$) and $\nabla^2$SST (contours). All these quantities are averaged over years 17–20 and spatially high-pass filtered with the two dimensional Hann filter, of the CFES integration. (d) Joint probability density function (PDF;%) of $\nabla^2$SST and wind stress curl. (e) PDFs of wind stress curl. Red (blue) histogram shows the PDF for positive (negative) $\nabla^2$SST larger (smaller) than 0.15 (−0.15) × $10^{-10}$C°$m^{-2}$.

equatorward propagation of jet-like features (Figure 4b) that overall corresponds well with the simulated depth-integrated zonal flow (Figure 4a), another indication of coupling between the deep zonal jets and SST induced fine-scale wind curls.

## 6. Conclusion and Discussion

[16] The present study examines oceanic deep zonal jets in the subtropical south Pacific simulated in a high-resolution atmosphere-ocean coupled GCM (CGCM). Its ability to simulate the jets enables the investigation of their air-sea interaction aspects, which has not been possible in past studies using ocean-only GCMs. Our analysis suggests that the deep zonal jets and the overlying fine-scale wind-stress curl field feed back positively onto each other by the following sequence of processes. First, the banded structures of barotropic zonal currents are generated due to some oceanic process(es) expressed as curl $\tau^{NL}$ in equation (2). These barotropic jets then generate SST anomalies with the latitudinal scale of a few degrees, then the ABL responds thermally to the SST anomalies and induces fine-scale wind stress anomaly via the atmospheric pressure adjustment mechanism. The meridional gradient of this fine-scale wind stress field in turn reinforces the original deep zonal jets via the Sverdrup dynamics, contributing up to about 50% of the simulated fine-scale zonal transport.

[17] The mid-basin bands of alternating jets simulated in CFES are not located exactly at the same latitudes as observed by KG06. However, the discrepancy in the location between the observation and the model rather provides a unique piece of evidence that the fine-scales KG06 found in the wind field is unlikely an artifact of the satellite scatterometer observation (e.g., during heavy rains); that is, the correspondence at fine-scales reported by KG06 between the oceanic geostrophic flow and the wind field is not a coincidence but a real phenomenon that can happen through air-sea interaction.

[18] It has been discussed that SST-induced, surface wind stress perturbations can feedback on to the ocean at oceanic mesoscales via Ekman pumping (e.g., see *Small et al.* [2008] and *Chelton and Xie* [2010] for reviews). The present study

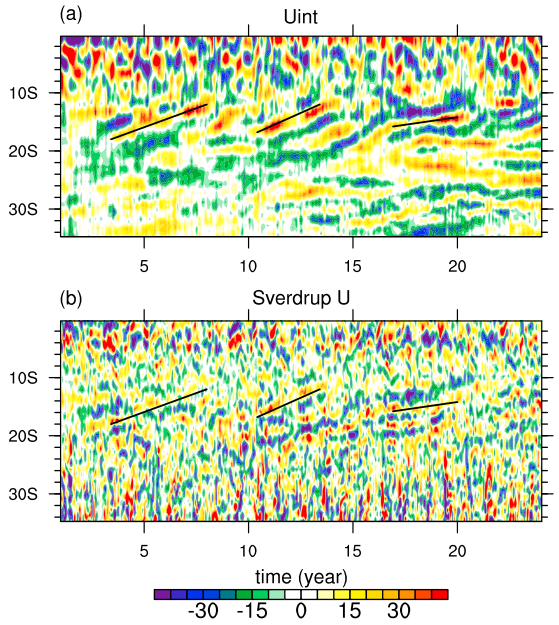


**Figure 4.** Latitude-time section of monthly mean (a) depth-integrated zonal velocity (unit in $m^2\ s^{-1}$) and (b) Sverdrup transport ($m^2\ s^{-1}$) averaged over 150°–110°W from the CFES integration. Black line segments represent the equatorward propagation of phase at 0.46 cm $s^{-1}$, 0.56 cm $s^{-1}$, and 0.18 cm $s^{-1}$, respectively from left to right.

possibly provides another example of SST-induced feedback to the ocean, acting as a positive feedback sustaining not only surface currents but also the bands of deep zonal flows. While the process initially generating the deep zonal jets is unidentified, our analysis suggests that air-sea interaction plays a role in generating fine-scale wind curl and in sustaining or reinforcing the oceanic deep jets largely in a manner consistent with the Sverdrup dynamics. To test the robustness of the positive feedback proposed in this study, targeted experiments with CFES and diagnosis of observational data and other high-resolution CGCMs are necessary.

[19] **Acknowledgments.** The integration of the CFES was carried out on the Earth Simulator under the support of JAMSTEC. We thank two anonymous reviewers for their constructive comments. Billy Kessler also provided a number of insightful comments. Thanks are extended to Nikolai Maximenko, Oleg Melnichenko, Shoshiro Minobe, Kelvin Richards, and Shang-Ping Xie for helpful discussions. A part of this work was conducted when BT visited IPRC during winter of 2010-11 under JAMSTEC-IPRC initiative. All the authors but RF are supported by MEXT through a Grant-in-Aid for Scientific Research in Innovative Areas 2205, and JSPS through KAKENHI 21540458 (BT and MN), 23340139 (BT and HS), and 22244057 (NK and AKY). RF is supported by JAMSTEC, by NASA through grant NNX07AG53G, and by NOAA through grant NA09OAR4320075. IPRC/SOEST contribution 863/8580.

[20] The Editor thanks two anonymous reviewers for their assistance in evaluating this paper.

## References

Chelton, D. B., and S.-P. Xie (2010), Coupled ocean-atmosphere interaction at oceanic mesoscales, *Oceanography*, *23*, 52–69.

Chelton, D. B., M. G. Schlax, M. H. Freilich, and R. F. Milliff (2004), Satellite measurements reveal persistent small-scale features in ocean winds, *Science*, *303*, 978–983.

Divakaran, P., and G. B. Brassington (2011), Arterial ocean circulation of the southeast Indian Ocean, *Geophys. Res. Lett.*, *38*, L01802, doi:10.1029/2010GL045574.

Enomoto, T., A. Kuwano-Yoshida, N. Komori, and W. Ohfuchi (2008), Description of AFES 2: Improvements for high-resolution and coupled simulations, in *High Resolution Numerical Modelling of the Atmosphere and Ocean*, edited by K. Hamilton and W. Ohfuchi, pp. 77–97, Springer, New York.

Kessler, W. S., and L. Gourdeau (2006), Wind-driven zonal jets in the South Pacific Ocean, *Geophys. Res. Lett.*, *33*, L03608, doi:10.1029/2005GL025084.

Kessler, W. S., G. C. Johnson, and D. W. Moore (2003), Sverdrup and nonlinear dynamics of the Pacific equatorial currents, *J. Phys. Oceanogr.*, *33*, 994–1008.

Komori, N., K. Takahashi, K. Komine, T. Motoi, X. Zhang, and G. Sagawa (2005), Description of sea-ice component of Coupled Ocean-Sea Ice Model for the Earth Simulator (OIFES), *J. Earth Simul.*, *4*, 31–45.

Komori, N., A. Kuwano-Yoshida, T. Enomoto, H. Sasaki, and W. Ohfuchi (2008a), High resolution simulation of the global coupled atmospheric-ocean system: Description and preliminary outcomes of CFES (CGCM for the Earth Simulator), in *High Resolution Numerical Modelling of the Atmosphere and Ocean*, edited by K. Hamilton and W. Ohfuchi, pp. 241–260, Springer, New York.

Komori, N., W. Ohfuchi, B. Taguchi, H. Sasaki, and P. Klein (2008b), Deep ocean inertia-gravity waves simulated in a high-resolution global coupled atmosphere-ocean GCM, *Geophys. Res. Lett.*, *35*, L04610, doi:10.1029/2007GL032807.

Kuwano-Yoshida, A., T. Enomoto, and W. Ohfuchi (2010), An improved PDF cloud scheme for climate simulations, *Q. J. R. Meteorol. Soc.*, *136*, 1583–1597.

Lebedev, K. V., S. DeCarlo, P. W. Hacker, N. A. Maximenko, J. T. Potemra, and Y. Shen (2010), Argo Products at the Asia-Pacific Data-Research Center, *Eos Trans. AGU*, *91*(26), Ocean Sci. Meet. Suppl., Abstract IT25A-01.

Lindzen, R. S., and S. Nigam (1987), On the role of sea surface temperature gradients in forcing low level winds and convergence in the tropics, *J. Atmos. Sci.*, *44*, 2418–2436.

Maximenko, N. A., B. Bang, and H. Sasaki (2005), Observational evidence of alternating zonal jets in the world ocean, *Geophys. Res. Lett.*, *32*, L12607, doi:10.1029/2005GL022728.

Maximenko, N. A., O. V. Melnichenko, P. P. Niiler, and H. Sasaki (2008), Stationary mesoscale jet-like features in the ocean, *Geophys. Res. Lett.*, *35*, L08603, doi:10.1029/2008GL033267.

Melnichenko, O. V., N. A. Maximenko, N. Schneider, and H. Sasaki (2010), Quasi-stationary striations in basin-scale oceanic circulation: Vorticity balance from observations and eddy-resolving model, *Ocean Dyn.*, *60*, 653–666, doi:10.1007/s10236-009-0260-z.

Minobe, S., A. Kuwano-Yoshida, N. Komori, S.-P. Xie, and R. Small (2008), Influence of the gulf stream on the troposphere, *Nature*, *452*, 206–209.

Nakano, H., and H. Hasumi (2005), A series of zonal jets embedded in the broad zonal flows in the Pacific obtained in eddy-permitting ocean general circulation models, *J. Phys. Oceanogr.*, *35*, 474–488.

Qiu, B., S. Chen, and W. S. Kessler (2009), Source of the 70-day mesoscale eddy variability in the Coral Sea and the North Fiji Basin, *J. Phys. Oceanogr.*, *39*, 404–420.

Richards, K. J., N. A. Maximenko, F. O. Bryan, and H. Sasaki (2006), Zonal jets in the Pacific Ocean, *Geophys. Res. Lett.*, *33*, L03605, doi:10.1029/2005GL024645.

Richards, K. J., H. Sasaki, and F. O. Bryan (2008), Jets and waves in the Pacific Ocean, in *High-Resolution Numerical Modelling of the Atmosphere and Ocean*, edited by K. Hamilton and W. Ohfuchi, pp. 182–196, Springer, New York.

Small, R. J., S. deSzoeke, S. P. Xie, L. O'Neill, H. Seo, Q. Song, P. Cornillon, M. Spall, and S. Minobe (2008), Air-sea interaction over ocean fronts and eddies, *Dyn. Atmos. Oceans*, *45*, 274–319.

Vallis, G. K. (2006), *Atmospheric and Oceanic Fluid Dynamics: Fundamentals and Large-scale Circulation*, 745 pp., Cambridge Univ. Press, Cambridge, U. K.

Webb, D. J. (2000), Evidence for shallow zonal jets in the South Equatorial Current region of the southwest Pacific, *J. Phys. Oceanogr.*, *330*, 706–720.

Xie, S. P., W. T. Liu, Q. Liu, and M. Nonaka (2001), Far-reaching effects of the Hawaiian Islands on the Pacific ocean-atmosphere system, *Science*, *292*, 2057–2060.

R. Furue, International Pacific Research Center, University of Hawai'i at Mānoa, 1680 East-west Rd., Honolulu, HI 96822, USA. (furue@hawaii.edu)

N. Komori, A. Kuwano-Yoshida, W. Ohfuchi, H. Sasaki, and B. Taguchi, Earth Simulator Center, Japan Agency for Marine-Earth Science and Technology, 3173-25 Showa-machi, Kanazawa-ku, Yokohama, Kanagawa 236-0001, Japan. (komori@jamstec.go.jp; akiray@jamstec.go.jp; ohfuchi@jamstec.go.jp; sasaki@jamstec.go.jp; bunmei@jamstec.go.jp)

M. Nonaka, Research Institute for Global Change, Japan Agency for Marine-Earth Science and Technology, 3173-25 Showa-machi, Kanazawa-ku, Yokohama, Kanagawa 236-0001, Japan. (nona@jamstec.go.jp)